Real-Time Spatial Estimates of Snow-Water Equivalent (SWE)

Sierra Nevada Mountains, California

February 7, 2018

Team: Noah Molotch[1,2], Leanne Lestak[1], Dominik Schneider[1], and Keith Musselman[1]
[1] Center for Water Earth Science & Technology, Institute of Arctic and Alpine Research, University of Colorado Boulder
[2] Jet Propulsion Laboratory, California Institute of Technology
Contact: Leanne.Lestak@colorado.edu

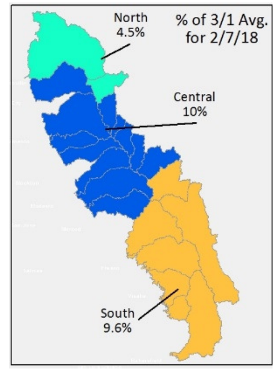

Summary of current conditions

The map on the right shows mean spatial SWE above 5000' and corresponds to a daily map released by the CA DWR, which uses snow sensor data. This map only includes the Feather and the Truckee in the North.

About this report

This is an product that provides near-real-time (NRT) estimates of snow-water equivalent (SWE) at a spatial resolution of 500 m for the Sierra Nevada in California over the latter portion of the snow season (February—June), approximately every 2 weeks. Due to processing time, this report will typically be released 2-3 days after the date at the top of the report. A similar experimental research product, covering the Intermountain West, makes its debut this season and will be distributed to water managers in Colorado, Utah and Wyoming.

The spatial SWE analysis method for the Sierra Nevada uses the following data as inputs:

- Operationally measured in-situ SWE from all CA snow gage sensor sites that have data available
- NRT MODSCAG (per pixel fractional snow-covered area or fSCA) data from the most recent cloud-free MODIS satellite image
- Physiographic information (elevation, latitude, upwind mountain barriers, slope, etc.)
- Historical daily SWE patterns (2000-2014) retrospectively generated using historical MODSCAG data, and an energy-balance model that back-calculates SWE given the fSCA timeseries and meltout date for each pixel

The use of historical SWE patterns provides more accurate estimation of current SWE than a method that interpolates between snow sensor sites using physiographic information alone (Schneider and Molotch, 2016). This method also allows for estimation of SWE values for elevations below and above the elevational extent of the snow gage sensor network. For more details on the estimation method, see the Methods section below.

Data availability for this report

93 snow gage sites in the Sierra Nevada network were recording SWE values out of a total of 114 sites. The locations of sensors that aren't recording snow (shown in yellow in Figure 3, left map) are lower elevation, southern latitude, and a few that are offline in other strategic locations. Eg. out of 114 sites, 93 were reporting SWE on the ground; 7 were reporting but had zero SWE; and 14 were offline

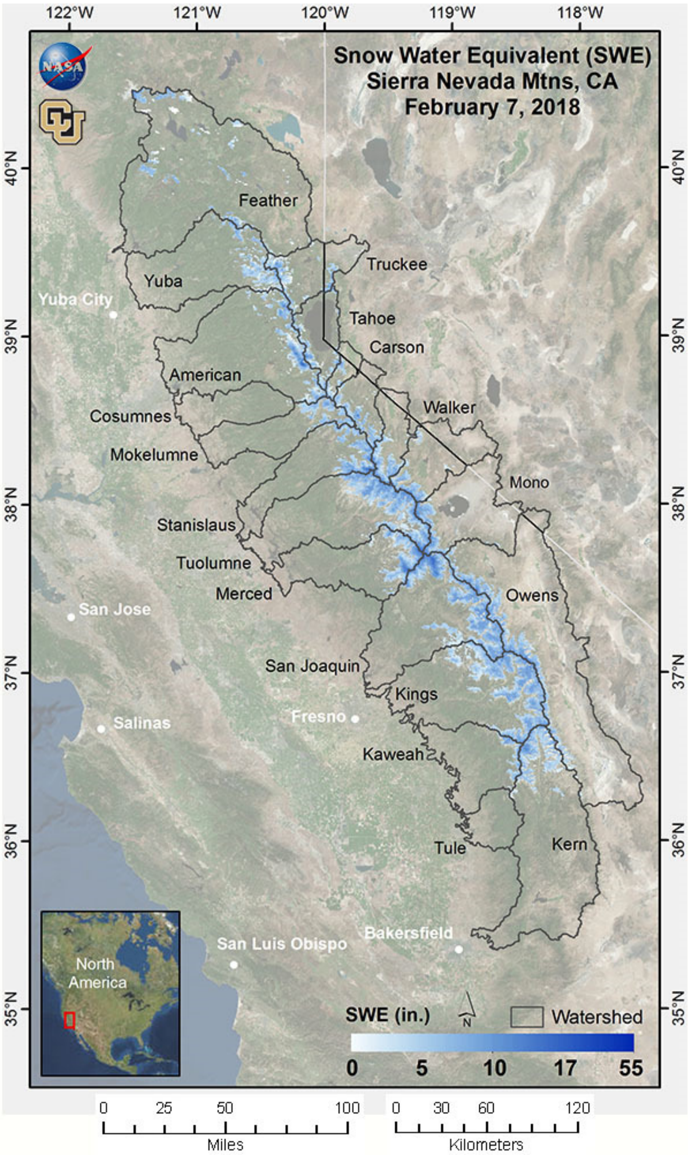

Figure 1. Estimated SWE across the Sierra Nevada. *SWE amounts for February 7, 2018 are shown.*

The value of spatially explicit estimates of SWE

Snowmelt makes up the large majority (~60-85%) of the annual streamflow in the Sierra Nevada. The spatial distribution of snow-water equivalent (SWE) across the landscape is complex. While broad aspects of this spatial pattern (e.g., more SWE at higher elevations and on north-facing exposures) are fairly consistent, the details can vary a lot from year to year, influencing the magnitude and timing of snowmelt-driven runoff.

SWE is operationally monitored at just over a hundred snow gage sensor sites spread across the Sierra Nevada, providing a critical first-order snapshot of conditions, and the basis for runoff forecasts from the CA DWR and NOAA. However, conditions at snow sensor sites (e.g., percent of normal SWE) may not be representative of conditions in the large areas between these point measurements, and at elevations above and below the range of the sensor sites. The spatial snow analysis creates a detailed picture of the spatial pattern of SWE using snow sensors, satellite, and other data, extending beyond the snow sensor sites to the unsampled areas. This makes it possible to identify unusual spatial patterns, and if significant differences from sensor-observed SWE conditions are present. More generally, the spatial snow analysis clearly shows the dynamic nature of the snow-water resource across both time and space.

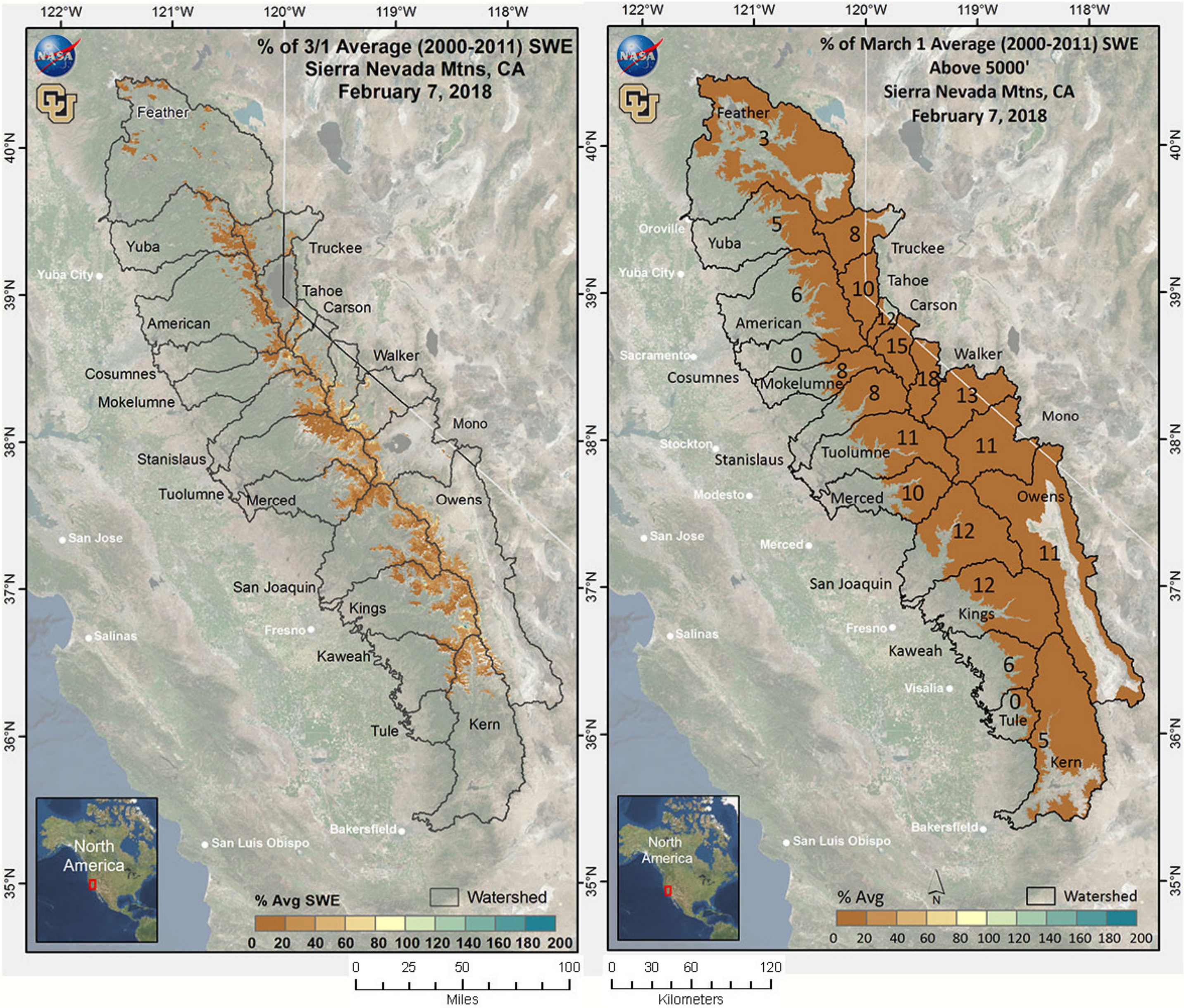

Figure 2*. *Estimated % of average SWE across the Sierra Nevada. *Percent of average (2000-2011) SWE for February 7, 2018 for the Sierra Nevada, calculated for each pixel (left) and basinwide (right). Basinwide percent of average is calculated across all model pixels >5000' elevation.*

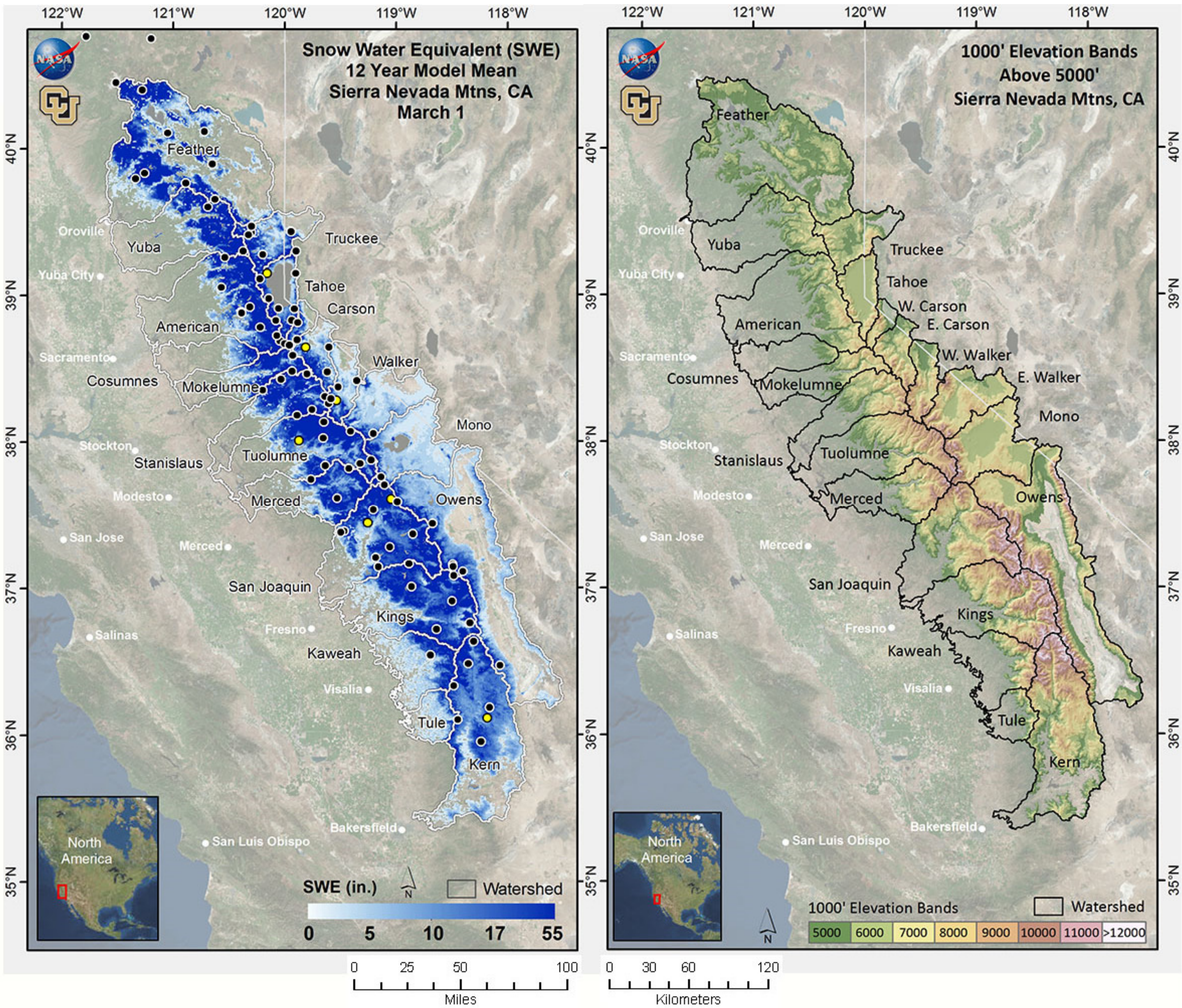

Figure 3. Mean SWE and Elevation Bands for the Sierra Nevada. *Mean SWE (2000-2011) amounts for March 1st (left), and Banded Elevation map identifies basins used in this report (black boundaries) and 1000' elevation bands (colored shading) that match those used in Table 1 and Table 2. Map on left shows snow gage sensor sites recording SWE on February 7, 2018 (black) and sites that had zero SWE are shown in yellow.*

Methods

The spatial SWE estimation method is described in Schneider and Molotch (2016). The method uses linear regression in which the dependent variable is derived from the operationally measured in situ SWE from all online snow sensor sites in the domain. The snow sensor SWE observations are scaled by the fractional snow-covered area across the 500 m pixel containing that snow sensor site before being used in the linear regression model.

The following independent variables (predictors) enter into the linear regression model:

- A near-real-time cloud-free MODIS satellite image which has been processed using the MODIS Snow Cover and Grain size (MODSCAG) fractional snow-covered area algorithm program (Painter, et. al. 2009, snow.jpl.nasa.gov)
- Physiographic variables that affect snow accumulation, melt, and redistribution, including elevation, latitude, upwind mountain barriers, slope, etc. See Figure 2 in Schneider and Molotch (2016) for the full set of these variables.
- The historical daily SWE pattern (2000-2014) retrospectively generated using historical MODSCAG data, and an energy-balance model that back-calculates SWE given the fractional Snow-Covered Area (fSCA) time series and meltout date for each pixel. See Guan, et. al., 2013 and the additional references for details. (For computational efficiency, only one image from either the 1st or 15th of each month during the 2000-2014 period that best matches the real-time snow sensor-observed pattern is selected as an independent variable.)

The real-time regression model for this date has been validated by cross-validation, whereby 10% of the snow sensor data are randomly removed and the model prediction is compared to the measured value at the removed snow sensor stations. This is repeated 30 times to get an average R-squared value, which denotes how closely the model fits the snow sensor data. During development of this regression method in the Intermountain West, the model was also validated against independent SWE data collected in NRCS snow surveys at 9 locations in Colorado and an intensive field survey in north-central Colorado.

Table 1. Estimated SWE by basin. *The basinwide SWE values and averages, are across all pixels at elevations >5000'. Shown are February 7th percent of March 1st average (between 2000-2011) SWE and mean SWE summarized for each basin.*

Basin	2/7/18 % 3/1 Avg to Date	2/7/18 SWE (in)
American	5.7	1.7
Cosumnes	0.4	0.1
E Carson	15.3	1.6
E Walker	13.2	0.8
Feather	3.1	0.5
Kaweah	5.6	1.2
Kern	5.2	0.7
Kings	11.7	2.8
Merced	9.5	2.2
Mokelumne	8.1	2.1
Mono	10.6	0.8
Owens	11.3	1.0
San Joaquin	11.9	2.9
Stanislaus	8.1	2.1
Tahoe	9.6	2.1
Truckee	8.3	1.2
Tule	0.3	0.0
Tuolumne	11.3	3.0
W Carson	12.2	1.9
W Walker	18.5	1.8
Yuba	5.5	1.7

Table 2. Estimated SWE by basin and elevation band. *Elevation bands begin at 5000' and extend past the highest point in the basin. Note that the area of the highest 2-5 bands is typically much smaller than the lower bands. Shown are February 7th percent of March 1st average (between 2000-2011) SWE and mean SWE summarized for each 1000' elevation band inside each basin.*

Basin	Elevation Band	2/7/18 % 3/1 Avg to Date	2/7/18 SWE (in)	Area Sq Mi
American	5000-6000'	0	0.0	295.5
	6000-7000'	2	0.7	261.0
	7000-8000'	9	3.6	166.3
	8000-9000'	16	7.1	67.8
	9000-10,000'	18	9.4	8.6
Cosumnes	5000-6000'	0	0.0	57.9
	6000-7000'	0	0.1	22.9
	7000-8000'	2	0.9	6.4
E. Carson	5000-6000'	0	0.0	65.9
	6000-7000'	0	0.0	90.7
	7000-8000'	4	0.5	104.8
	8000-9000'	19	3.1	95.2
	9000-10,000'	33	6.3	33.8
	10,000-11,000'	39	7.6	10.3
	> 11,000'	27	8.1	0.3
E. Walker	5000-6000'	0	0.0	21.5
	6000-7000'	0	0.0	211.7
	7000-8000'	0	0.0	254.4
	8000-9000'	4	0.3	185.8
	9000-10,000'	27	3.4	76.6
	10,000-11,000'	31	7.3	40.6
	11,000-12,000'	32	8.2	10.3
	> 12,000'	32	8.5	0.3
Feather	5000-6000'	1	0.1	1,259.3
	6000-7000'	4	0.8	706.5
	7000-8000'	12	2.8	114.3
	8000-9000'	23	7.0	3.7
Kaweah	5000-6000'	0	0.0	62.1
	6000-7000'	0	0.0	59.5
	7000-8000'	0	0.0	58.6
	8000-9000'	2	0.4	55.6
	9000-10,000'	9	2.4	43.6
	10,000-11,000'	16	6.6	29.8
	11,000-12,000'	17	7.9	8.1
	> 12,000'	17	7.8	0.2
Kern	5000-6000'	0	0.0	294.4
	6000-7000'	0	0.0	369.9
	7000-8000'	0	0.0	336.4
	8000-9000'	0	0.0	315.5
	9000-10,000'	3	0.5	187.5
	10,000-11,000'	15	3.1	127.9
	11,000-12,000'	21	6.3	92.8
	> 12,000'	28	8.1	44.2

Kings	5000-6000'	0	0.0	101.3
	6000-7000'	0	0.0	131.6
	7000-8000'	0	0.0	168.6
	8000-9000'	3	0.6	216.8
	9000-10,000'	13	2.8	209.7
	10,000-11,000'	20	6.0	189.6
	11,000-12,000'	23	8.0	150.5
	> 12,000'	24	8.8	51.2
Merced	5000-6000'	0	0.0	70.3
	6000-7000'	0	0.0	78.2
	7000-8000'	0	0.1	135.0
	8000-9000'	9	1.9	118.6
	9000-10,000'	21	5.7	83.2
	10,000-11,000'	20	8.9	37.3
	11,000-12,000'	20	10.8	11.5
	> 12,000'	19	12.1	1.4
Mokelumne	5000-6000'	0	0.0	81.0
	6000-7000'	0	0.1	63.8
	7000-8000'	6	1.9	87.0
	8000-9000'	19	5.7	75.4
	9000-10,000'	23	8.0	7.9
Mono	6000-7000'	0	0.0	378.1
	7000-8000'	0	0.0	396.2
	8000-9000'	2	0.1	175.3
	9000-10,000'	22	3.0	63.0
	10,000-11,000'	25	7.6	45.8
	11,000-12,000'	25	8.9	25.8
	> 12,000'	26	9.2	4.5
Owens	5000-6000'	0	0	424.2
	6000-7000'	0	0	412.9
	7000-8000'	0	0.0	462.7
	8000-9000'	2	0.2	258.5
	9000-10,000'	11	1.2	190.4
	10,000-11,000'	20	3.4	195.1
	11,000-12,000'	24	5.8	145.5
	> 12,000'	25	6.5	79.9
San Joaquin	5000-6000'	0	0.0	141.0
	6000-7000'	0	0.0	179.5
	7000-8000'	0	0.1	211.4
	8000-9000'	7	1.5	194.4
	9000-10,000'	16	4.5	199.7
	10,000-11,000'	20	7.2	157.9
	11,000-12,000'	20	8.6	116.7
	> 12,000'	23	9.0	25.8

Stanislaus	5000-6000'	0	0.0	105.5
	6000-7000'	0	0.0	134.9
	7000-8000'	3	0.7	142.9
	8000-9000'	17	4.9	112.9
	9000-10,000'	22	7.9	49.1
	10,000-11,000'	21	10.0	11.8
	> 11,000'	23	10.5	0.3
Tahoe	6000-7000'	1	0.2	319.0
	7000-8000'	7	1.7	105.7
	8000-9000'	15	4.5	68.4
	9000-10,000'	23	7.1	15.8
	10,000-11,000'	28	8.4	0.6
Truckee	5000-6000'	0	0.0	133.5
	6000-7000'	3	0.3	245.4
	7000-8000'	10	2.4	126.9
	8000-9000'	20	5.0	39.7
	9000-10,000'	30	7.3	9.4
	10,000-11,000'	35	8.6	0.4
Tule	5000-6000'	0	0.0	51.4
	6000-7000'	0	0.0	40.8
	7000-8000'	0	0.0	26.7
	8000-9000'	0	0.0	14.5
	9000-10,000'	4	0.9	4.3
	10,000-11,000'	17	4.1	0.1
Tuolumne	5000-6000'	0	0.0	167.2
	6000-7000'	0	0.0	139.8
	7000-8000'	2	0.5	150.0
	8000-9000'	12	3.7	164.1
	9000-10,000'	18	6.3	173.0
	10,000-11,000'	22	8.3	87.1
	11,000-12,000'	24	9.5	23.9
	> 12,000'	22	10.3	2.8
W. Carson	5000-6000'	0	0.0	24.9
	6000-7000'	0	0.0	13.7
	7000-8000'	5	0.7	39.2
	8000-9000'	17	3.4	33.2
	9000-10,000'	25	6.6	11.1
	10,000-11,000'	23	7.7	1.1
W. Walker	5000-6000'	0	0	78.8
	6000-7000'	0	0.0	68.7
	7000-8000'	0	0.0	97.5
	8000-9000'	14	1.2	83.6
	9000-10,000'	26	5.6	73.5
	10,000-11,000'	26	8.0	28.8
	> 11,000'	30	8.3	2.3
Yuba	5000-6000'	0	0.0	191.7
	6000-7000'	5	1.7	214.6
	7000-8000'	12	4.3	110.0
	8000-9000'	21	8.2	3.8

Location of Reports and Excel Format Tables

ftp://snowserver.colorado.edu/pub/fromLeanne/forCADWR/Near_Real_Time_Reports/

References

Guan, B., N. P. Molotch, D. E. Waliser, S. M. Jepsen, T. H. Painter, and J. Dozier. (2013). Snow water equivalent in the Sierra Nevada: Blending snow sensor observations with snowmelt model simulations. *Water Resources Research, Vol. 49, 5029–5046, doi:10.1002/wrcr.20387.*

Painter, T.H., K. Rittger, C. McKenzie, P. Slaughter, R. E. Davis and J. Dozier. (2009) Retrieval of subpixel snow covered area, grain size, and albedo from MODIS. *Remote Sensing of the Environment*, 113: 868-879.

Schneider D. and N.P. Molotch. (2016). Real-time estimation of snow water equivalent in the Upper Colorado River Basin using MODIS-based SWE reconstructions and SNOTEL data. *Water Resources Research*, 52(10): 7892-7910. DOI: 10.1002/2016WR019067.

Additional Historical Reconstructed SWE Sources

Molotch, N.P. (2009). Reconstructing snow water equivalent in the Rio Grande headwaters using remotely sensed snow cover data and a spatially distributed snowmelt model. *Hydrological Processes*, Vol. 23, doi: 10.1002/hyp.7206, 2009.

Molotch, N.P., and S.A. Margulis. (2008) Estimating the distribution of snow water equivalent using remotely sensed snow cover data and a spatially distributed snowmelt model: a multi-resolution, multi-sensor comparison. *Advances in Water Resources*, 31, 2008.

Molotch, N.P., and R.C. Bales. (2006). Comparison of ground-based and airborne snow-surface albedo parameterizations in an alpine watershed: impact on snowpack mass balance. *Water Resources Research*, VOL. 42, doi:10.1029/2005WR004522.

Molotch, N.P., and R.C. Bales. (2005). Scaling snow observations from the point to the grid-element: implications for observation network design. *Water Resources Research*, VOL. 41, doi: 10.1029/2005WR004229.

Molotch, N.P., T.H. Painter, R.C. Bales, and J. Dozier. (2004). Incorporating remotely sensed snow albedo into a spatially distributed snowmelt model. *Geophysical Research Letters*, VOL. 31, doi:10.1029/2003GL019063, 2004.